Eur. Phys. J. D **9**, 49–54 (1999)

THE EUROPEAN PHYSICAL JOURNAL D

EDP Sciences

Production and stability of silicon-doped heterofullerenes

M. Pellarin[1,a], C. Ray[1], J. Lermé[1], J.L. Vialle[1], M. Broyer[1], X. Blase[2], P. Kéghélian[2], P. Mélinon[2], and A. Perez[2]

[1] Laboratoire de Spectrométrie Ionique et Moléculaire (U.M.R. 5579) 43, B[ld] du 11 Novembre 1918, F-69622 Villeurbanne Cedex, France

[2] Département de Physique des Matériaux (U.M.R. 5586) 43, B[ld] du 11 Novembre 1918, F-69622 Villeurbanne Cedex, France

Received: 1 September 1998 / Received in final form: 21 October 1998

Abstract. Silicon–carbon binary clusters with various mean compositions are generated in a laser vaporization source from targets processed as mixtures of graphite and silicon powders. Their size distribution is first analyzed by time-of-flight mass spectroscopy, which shows the stability of carbon fullerenes doped with silicon atoms in substitutional sites. Further investigations on the level of silicon doping are carried out by means of the laser-induced fragmentation of selected sizes. The photoproduct size distributions give evidence for at least nine silicon atoms substituted into still stable fullerene networks. The synthesis of heterofullerenes is mainly assisted by the nucleation mechanisms from Si−C mixed atomic vapors. Just as in the case of externally doped fullerene precursors, the laser-induced annealing of stoichiometric silicon-carbide clusters appears as an alternative route to produce heterofullerenes in the gas phase.

PACS. 36.40.-Qv Stability and fragmentation of clusters

1 Introduction

Doping fullerenes with foreign atoms are of main interest for their ability to be assembled into materials with specific physical and chemical properties. Since the discovery [1] and the large scale synthesis of fullerenes [2], numerous experimental and theoretical studies have been devoted to endohedrally doped (where a foreign atom is inside the cage) [3, 4] and exohedrally doped (where a foreign atom is outside the cage) fullerenes [5, 6]. The third possibility, trapping the foreign atoms as a part of the fullerene network, is also very promising because it induces a strong modification of their electronic properties while retaining the roughly spherical cage structure [7]. In gas phase experiments, substitution can be achieved either by the annealing of externally coated fullerene precursors [8, 9] or by a direct growth from mixtures of carbon and doping elements.

The substitutional doping is expected to be easier with elements disclosing a more favorable covalent bonding character rather than metals. For instance, since boron nitride is isoelectronic to graphite, the boron–nitrogen analogues of carbon nanotubes give a hint of the possibility of producing B-doped or N-doped heterofullerenes. Guo *et al.* have succeeded in showing that up to six boron atoms can be substituted into the carbon fullerene network [10]. This work has initiated much experimental effort in the field of the synthesis and characterization of boron- [11] and nitrogen-doped [12–15] fullerenes, which can be isolated in macroscopic quantities. Numerous theoretical studies have also been devoted to the electronic structure of such clusters [16–19] and their dimers [20–22]. A major interest is their specific electronic properties, since B- and N-doped atoms are found responsible for impurity electronic states similar to acceptor and donor levels in semi-conductors [23, 24]. Similar properties should be induced by silicon doping; silicon is the most logical candidate, since it is isoelectronic to carbon. Although silicon is known to prefer sp^3-like bonding and three-dimensional atomic arrangements, the stability of heterofullerenes doped with one silicon atom has been evidenced in mass abundance spectroscopy [25] and mobility measurements [26]. Further mass spectroscopy and photofragmentation studies have shown the stability of $C_{2n-2}Si_2^+$ clusters and the closeness of silicon atoms in the carbon network, in agreement with *ab initio* calculations [27]. It will now be interesting to see to what extent silicon atoms can be substituted without destroying the cage-like atomic arrangements, and how the doped atoms fit in these heterofullerenes.

2 Experimental setup

Mixed clusters are produced in a standard laser vaporization source from mixed Si_xC_{1-x} targets consisting of composite rods processed by binding silicon and graphite powders in various proportions [28]. In the case $x = 50\%$, which corresponds to the stoichiometric silicon–carbide phase, we use a commercial monocrystalline rod. A pulsed high-

[a] e-mail: pellarin@hplasim2.univ-lyon1.fr

pressure helium burst ensures the cluster growth in the source chamber from the plasma generated by the focused beam of an Nd:YAG laser (532 nm, 10 Hz). The cluster size distribution is then studied by a reflectron time-of-flight (RTOF) spectrometer set perpendicular to the incoming cluster beam (described elsewhere [29]). The neutral clusters are photoionized by an ArF excimer laser at a fixed photon energy of 6.4 eV. The laser fluence can be increased to induce multiphoton ionization processes and subsequent warming and dissociation of initially cold clusters. On the other hand, clusters directly born as ions in the source are analyzed by a suited triggering of pulsed high voltages applied onto the grids of the accelerating system (Wiley–Mc Laren configuration). Photo-fragmentation (PF) experiments on selected cluster sizes can be realized by taking advantage of the reflectron geometry in a tandem TOF analysis. After being accelerated in the free-flight zone of the spectrometer, clusters of a given mass are selected by an electrostatic gate and shined by the focused beam of a XeCl excimer laser (4.03 eV). The resolution of the mass selection is about $M/\Delta M \cong 170$. The charged products evaporated from the heated clusters during the remaining flight time up to the grounded entrance grid of the reflector are dispersed in their returning path to the detector. The fragmentation mass spectra will be insensitive to the dissociation processes occurring in the reflection and returning stages. To allow the detection of photoproducts with small sizes as compared to their parents, the reflector voltages can be consequently decreased for a better mass resolution.

3 Mass spectroscopy measurements

The size distribution of positively charged and neutral C_nSi_m clusters is first analyzed by TOF spectroscopy.

3.1 Positively charged mixed clusters with different compositions

Figure 1 gives mass spectra of $C_nSi_m^+$ clusters grown as positive ions for several target compositions in the region of the C_{60} fullerene. The almost pure carbon cluster size distribution, for a very low silicon concentration ($x = 1\%$) mainly discloses the enhanced abundance of fullerene sizes, especially for C_{50}, C_{60} and C_{70} [1, 30]. With a stoichiometric target ($x = 50\%$) the mass spectrum is very congested, and consists of 4 a.m.u. distant clumps of peaks with decreasing intensities. This size distribution is expected from a statistical growth of SiC clusters with the same sticking probability for both elements, considering their natural isotopic distribution [27]. For a weak silicon doping ($x =$ 10% in Fig. 1), besides pure carbon fullerenes, one can observe the growth of two series of peaks assigned to one- and two-silicon-containing even-numbered clusters ($C_{2n-1}Si^+$ and $C_{2n-2}Si_2^+$), respectively. A relatively higher stability is found for clusters having the same total number of atoms as the fullerenes ($n = 50, 60$ and 70). This mirroring among

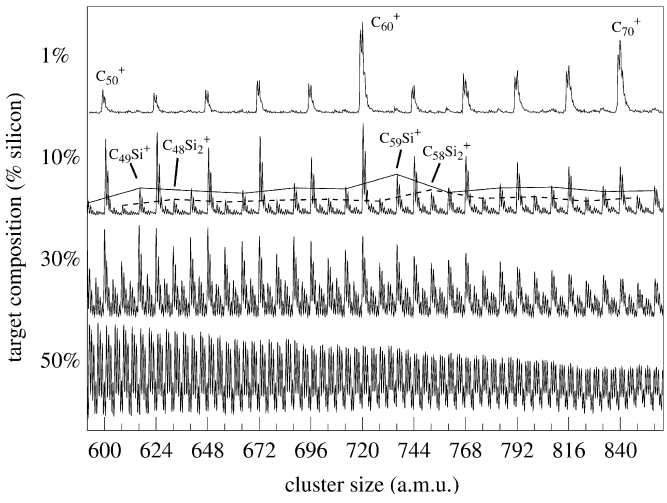

Fig. 1. TOF mass spectra of mixed $C_nSi_m^+$ clusters for different target compositions ($C_{1-x}Si_x$).The series $C_{2n-1}Si^+$ and $C_{2n-2}Si_2^+$ are connected by full and dotted lines in the case of $x = 10\%$.

the size distributions is an indication of the doping of silicon atoms in substitutional sites. The doping efficiency, which decreases with the number of Si atoms, seems to be statistical, although weaker than expected from the target composition. Unfortunately, if it exists, the small amount of more doped species ($C_{2n-7}Si_3^+$,...) is superimposed onto the main series because of the 3/7 ratio between the masses of the ^{12}C and ^{28}Si, the most abundant isotopes. For a larger composition of silicon ($x = 25\%$ in Fig. 1), it is now difficult to make a distinction among the three series that have similar intensities. This indicates an increasing overlap of cluster series with more and more doped silicon. The heterofullerene structure is nevertheless preserved, because of the even numbering of these clusters reflected in the outstanding spacing of 8 a.m.u. between successive clumps. This is totally different from the case of stoichiometric clusters ($x = 50\%$) where the 4 a.m.u. separation indicates the presence of odd-numbered species in comparable amount. As previously reported for pure carbon fullerenes [30], the size distribution of silicon-doped heterofullerenes is very dependent on the thermalization parameters in the laser vaporization source. A large time of residence in the nucleation chamber is necessary to promote the growth of the even-numbered clusters, to the detriment of silicon carbide-like clusters. For instance, a small amount of the latter is still present in the spectrum for $x = 25\%$.

3.2 Multiphoton ionization of neutral stoichiometric clusters

The size distribution of neutral clusters produced from a stoichiometric target ($x = 50\%$) is first analyzed at low ionizing laser fluence in order to avoid fragmentation in the TOF spectrometer. If enlarged, the one-photon spectrum of Fig. 2a is very similar to the one observed on direct ions ($x = 50\%$ in Fig. 1), and shows an appearance threshold

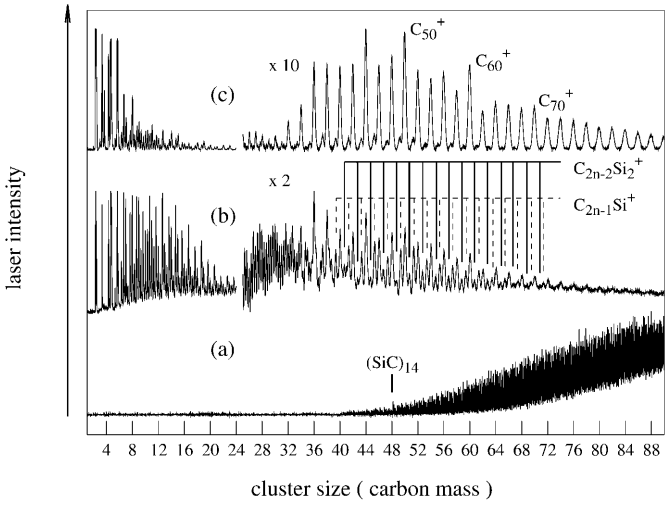

Fig. 2. Photoionization mass spectra of stoichiometric $(SiC)_n$ cluster ($x = 50\%$) at different laser fluences: (a) low laser fluence, high resolution spectrum (one-photon ionization); (b) intermediate laser fluence (the heterofullerene series $C_{2n-1}Si^+$ and $C_{2n-2}Si_2^+$ are indicated); (c) maximum laser fluence.

at this photon energy (6.4 eV), for a mean cluster size of about $(SiC)_{14}$. When the laser fluence is increased, ionized clusters undergo unimolecular evaporation processes in the ionization region, which modifies and shifts the size distribution towards small sizes. As further dissociation steps may occur in the RTOF and lead to a congestion of the mass spectra, they are recorded in an on-line configuration (at the cost of a lowering of mass resolution) so as to give a correct idea of the cluster distribution just at the end of the initial acceleration zone. At maximum laser fluence (Fig. 2c), the observed clusters are, surprisingly, almost pure carbon ones. Their size distribution is dominated by the fullerene sequence and very similar to what can be obtained if they were produced from a pure graphite target. At the intermediate laser fluence (Fig. 2b), additional peaks are present, and can be assigned to silicon-doped heterofullerenes just like in the case of the ions in Fig. 1. Intermediate spectra would show that the transition from the extreme situations (Fig. 2a,c) is gradual; the heterofullerene sizes first emerge from the background distribution of SiC stoichiometric clusters, and are progressively vanishing all the more rapidly, since they contain a large amount of silicon.

The multi-photon ionization spectra reflect the relative stability of ionized clusters similar to the way direct mass spectroscopy does on clusters directly born as cold ions. An increase of the laser fluence is equivalent to a decrease in the target doping with silicon. It therefore appears that, during the acceleration period that follows the laser ionization and warming, the initially stoichiometric clusters ($x = 50\%$) evaporate many more silicon than carbon atoms, and undergo a transformation from compact to cage-like structures. This process occurs in the opposite direction from the previously demonstrated transformation of metal-coated fullerenes into metal carbides [31].

4 Photofragmentation of selected sizes

More information about the laser annealing of stoichiometric clusters and the quantity of Si atoms that can be doped in the fullerene cages can be achieved in PF experiments on selected sizes.

4.1 Carbon-rich clusters

From targets processed with a not-too-large silicon concentration, it is possible to produce even-numbered mixed clusters that retain a heterofullerene structure, as presaged from Fig. 1. Mass coincidences hinder any confident estimation of the amount of silicon in these clusters. This difficulty can be partly passed over by analyzing the photoproduct size distribution that originates from clusters with different compositions inside a given mass bunch. As the photodissociation cross section is shown to strongly increase with the number of silicon-doped atoms, the PF spectra obtained at low laser fluence are expected to preferentially make the dissociation products from the most siliconized species appear. Regarding the case of a 25%-silicon-doped target: Fig. 3 gives the low fluence PF spectrum of clusters selected in the $\{C_{78}^+\}$ mass clump, which is expected to contain C_{78}^+, and eventually $C_{71}Si_3^+$, $C_{64}Si_6^+$, $C_{57}Si_9^+$,... sizes, in descending amount. Because the mass peak width (FWHM) that originates from the natural isotopic distribution is about 4 a.m.u., the resolution of the mass selector allows the isolation of this mass clump from its neighbors. Even if the pure fullerenes (C_{78}^+) are the most abundant precursors, their contribution is almost negligible here, and is restricted to the earliest C_2 losses [32, 33] observed in the right side of the spectrum. The size distribution is rather complicated, and results from the superimposition of the dissociation patterns of all present precursors containing at least three Si atoms. Nevertheless, the photoproducts are surprisingly all *even numbered* and will be assigned to the most likely heterofullerenes containing 0, 1, or 2 silicon atoms for simplicity, even if a small quantity of more largely doped clusters may be present but masked by the former ones.

In the case of $C_{2n-q}Si_q^+$ clusters with $q = 1$ or 2, the sequential dissociation always starts with the evaporation of the most silicon-containing dimer (Si_2 or SiC) as a first step. The C_2 loss has a higher activation energy, and occurs only after a complete elimination of silicon, just when the photoproducts have turned into pure carbon fullerene themselves [28]. Each of the three series then must not be considered as describing a sequential decay of C_2 dimers that would connect clusters having the same number of doped silicon atoms. The spectrum rather reflects the convolution of both the stability of the photoproducts and the stability of the neutral molecules involved in decay chains from the precursors. For instance, it will be shown in a forthcoming paper that, for more doped fullerenes ($q = 3$), the Si_3C and Si_2 neutral molecules are preferentially evaporated, while weak contributions of Si_2C_2 and SiC_3 products can be also detected. In this way, the largest peaks (C_{70}^+ and $C_{71}Si^+$) are explained by the Si_3C and

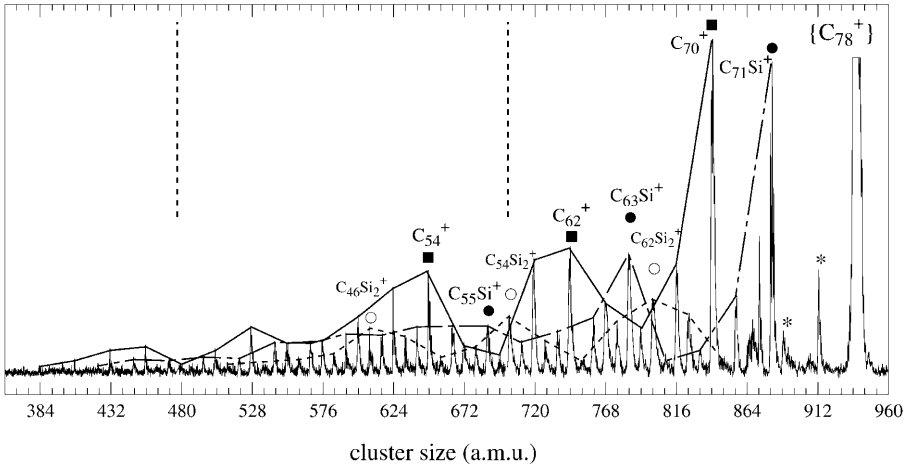

Fig. 3. Low fluence photofragmentation mass spectrum of clusters contained in the mass clump $\{C_{78}^+\}$ produced from a 25%-silicon-doped target. The photoproducts assigned to C_{2n}^+, $C_{2n-1}Si^+$, and $C_{2n-2}Si_2^+$ series are connected by full, dashed-dotted and dashed lines respectively. Their most prominent peaks are indicated by squares (■), dots (●), and circles (○). The stars (∗) locate the residual products of the C_{78}^+ selected clusters. The vertical dotted lines separate the three joined size domains recorded at different reflecting voltages.

Si_2 losses from the $C_{71}Si_3^+$ precursor. The step-like evaporation of these molecules should be responsible for the PF patterns of more Si-doped clusters selected in the same mass clump.

The most striking feature in this spectrum is the 96 a.m.u. progression in the size distribution of each photoproduct series, reflected in the large intensities for (C_{70}^+, C_{62}^+, C_{54}^+,...), ($C_{71}Si^+$, $C_{63}Si^+$, $C_{55}Si^+$,...) or ($C_{62}Si_2^+$, $C_{54}Si_2^+$, $C_{48}Si_2^+$..) clusters, which are not expected to be especially stable with regard to their total number of atoms. This general behavior is not related to a particular sequential decay, because the three series do not decay independently from one another, and may be connected by the loss of silicon-containing molecules, and because a C_8 loss (96 a.m.u.) is unlikely, at least for pure fullerenes [32–34]. A better explanation can be found when one notices that all the clusters selected at the same time, C_{78}^+, $C_{71}Si_3^+$, $C_{64}Si_6^+$, $C_{57}Si_9^+$,..., differ mainly by stepped amounts of *three* Si atoms. If one of these clusters evaporates an Si_3C molecule, which is a major dissociation channel, as seen above, it turns into a cluster with the same number of Si atoms as its predecessor in the list, and is expected to further dissociate in the same way, although the number of carbon atoms is different. This has been verified by observing that, under the same experimental conditions (laser fluence), the PF spectra of any $\{C_{2n}^+\}$ clumps that differ only by their number of carbon atoms are indeed quite similar. The shifts of 96 a.m.u. would then mainly originate from the contributions to the whole dissociation sequence of the successive precursors containing more and more silicon. For example, the C_{70}^+, C_{62}^+, C_{54}^+ products are well described by the single, double, or triple Si_3C losses from $C_{71}Si_3^+$, $C_{64}Si_6^+$ and $C_{57}Si_9^+$, respectively. The situation is actually made more complicated by the existence of competing dissociation pathways, and the intense peaks at $C_{71}Si^+$, $C_{63}Si^+$, $C_{55}Si^+$ can be understood from the cumulate losses of Si_2, Si_2+Si_3C, Si_2+Si_3C+Si_3C from $C_{71}Si_3^+$, $C_{64}Si_6^+$ and $C_{57}Si_9^+$. $C_{64}Si_2^+$ and $C_{62}Si_2^+$ also originate in the Si_2+Si_2 or Si_2+Si_2C_2 decays from $C_{64}Si_6^+$ and higher-order sequences involving an additional Si_3C loss from $C_{57}Si_9^+$ explain the signal rise in the vicinity of the $C_{54}Si_2^+$ product. For the same reasons, the absence of $C_{58}Si_2^+$ and $C_{65}Si^+$ products is well explained by the number of carbon atoms larger than the one contained inside their most likely precursors $C_{57}Si_9^+$ and $C_{64}Si_6^+$.

So, even if the involved dissociation pathways cannot be described precisely, the observation of successive shifts in the photoproduct size distributions is, however, an indication that even-numbered clusters containing up to nine Si atoms contribute to a fullerene-like fragmentation pattern. This is in favor of their arrangement as substitutionaly doped heterofullerenes.

4.2 Stoichiometric clusters

Multi-photon ionization mass spectra (Fig. 2) provide, for a given laser fluence, a photograph of the dissociation products that originate from all the silicon carbide cluster precursors shined by the laser. More precise information will be provided by the analysis of the photoproducts born from mass-selected clusters. Fig. 4 shows the PF spectra of five mass clumps selected in the size distribution of stoichiometric ions, as displayed in Fig. 1 ($x = 50\%$) and corresponding to the most likely compositions $(SiC)_{32}^+$, $(SiC)_{40}^+$, $(SiC)_{47}^+$, $(SiC)_{54}^+$ and $(SiC)_{62}^+$ (if a statistical growth mechanism is assumed). Several size domains are investigated by adjusting the reflector voltages, and the laser fluence is optimized to get the maximum signal in each of them. The first dissociation steps (right side of the spectra) can be precisely described as the sequential and bimodal evaporation of Si_2C and Si_3C neutral molecules with respective weights 0.7 and 0.3. Proceeding with increasing mass loss and after a region in which no

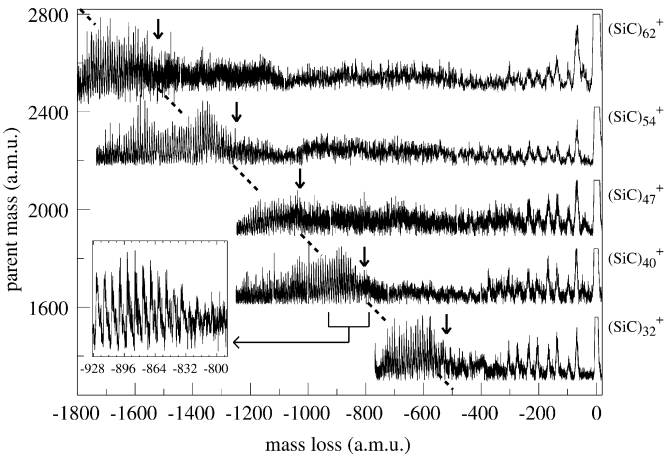

Fig. 4. Photofragmentation mass spectra of stoichiometric $(SiC)_n$ clusters ($x = 50\%$) for n around 32, 40, 47, 54, and 62. The onsets of heterofullerene products are indicated by arrows (their linear dependence with the precursor sizes is evidenced by a dotted line to guide the eyes). An enlarged portion of the second spectrum shows the 8 a.m.u. periodicity among heterofullerenes.

significant signal is detected, the onset of a second product size distribution (arrows in Fig. 4) is observed. They are all even numbered, and undoubtedly correspond to silicon-doped heterofullerenes, because of the 8 a.m.u. distance between consecutive peak clumps (inset in Fig. 4). A direct estimate of the silicon content is impossible because of mass coincidences. Nevertheless, a careful analysis shows that the mass loss at the onset of heterofullerene appearance does not depend on the laser fluence, and varies linearly with the precursor size (see the straight dotted line in Fig. 4). We will make the assumption that the selected clusters are nearly stoichiometric and that the earliest dissociation steps involve the statistical loss of Si_2C and Si_3C molecules ($Si_{2.3}C$ on the average) down to the transformation into heterofullerenes. In this case, and since the linear function does not go through zero, the hypothesis of a fixed critical Si/C atomic ratio for the heterofullerene stability must be eliminated. The experimental observations are rather consistent with a fixed number of silicon atoms remaining in the first appearing heterofullerene products. In the framework of a binomial distribution law, the composition of clusters selected in a mass bunch is slightly dispersed over the mean value ($x = 50\%$), and the rough number of 16 to 17 silicon atoms that can be deduced from the linear behavior (Fig. 4) is somewhat overestimated. Actually, the parent clusters that are slightly deficient in silicon contribute to a heterofullerene product distribution shifted to larger sizes, relative to the size expected for exactly stoichiometric clusters. Anticipating that clusters with a composition bracketed by the FWHM of the binomial distribution $x = 50\%$ contribute effectively to the heterofullerene fragment distribution, the remaining number of silicon atoms at the onset of heterofullerene products is more consistent with a corrected value close to 12. Since neither the initial cluster composition nor the pointing of the onsets are unambiguous, this value must be considered as a rough estimate. Moreover, no heterofullerene-like product can be detected for sizes below $(SiC)_{30}$. It seems that, even if a residual number of about 12 silicon atoms can be reached after several evaporation steps, the total number of remaining atoms (12 Si and 22 C on the average) is not sufficient to allow their arrangement in a cage-like structure. This value is strikingly close to limit for pure carbon fullerene stability (about $n = 32$).

The PF spectra are then qualitatively consistent with the preferential evaporation of silicon and the structural changes observed in photoionization spectra. For large enough precursor sizes and mass losses, PF spectra would display the progressive emergence of pure carbon fullerenes resulting from the further dissociation of heterofullerene products. The size distribution in the spectra of Fig. 2 is mainly explained by the presence of large neutral clusters produced in the source.

5 Conclusion

Photofragmention mass spectroscopy experiments have shown the possibility of a large doping of silicon atoms in the carbon fullerene networks. Silicon-doped fullerenes can originate either from the nucleation of mixed Si−C atomic vapors or from the transformation of initially stoichiometric species through laser heating. So different ways of synthesis enlighten the stability of heterofullerenes in the gas phase at the present experimental time scale (ms). It will be interesting to go further by achieving the isolation of these species by chemical means. In that respect, larger yields of heterofullerenes than those reached in this experiment are needed, and arc discharge techniques should be an alternative route to synthesizing them [2, 11]. Previous computational studies have pointed out the propensity of silicon atoms to be arranged as close neighbors and to induce nonnegligible deformations of the cages in their vicinity [28]. The popping out of Si atoms from the fullerene cage can be qualitatively explained by simple considerations of their larger atomic radius, the fact that Si−C bonds are longer than C−C bonds, and the requirement of an sp^3-like hybridization. Although such work could be extended to heterofullerenes with about ten Si-doped atoms, the stability of these heterofullerences is questionable precisely because of this feature, even when experimentally observed. Since experiment gives indications of a cage-like structure for these clusters, one can speculate that for a large number of Si doping atoms, the atomic arrangement no longer retains the conventional fullerene network (hexagons+12 pentagons) [35]. Among the various cage-like families of polyhedrons that can be generated by the Euler's theorem, the one obtained by replacing the 12 pentagonal cycles by 6 square ones is a potential candidate for a larger silicon substitution. Their lower symmetry, and the distortions induced by their square faces, make such structures unlikely for pure carbon clusters [36], but this can be an asset, for they receive substitutional silicon atoms. They have already been shown as an alternative form of the fullerenes in the case of boron nitride

(BN_n) clusters, since the even numbering of edges in each face allows the chemical alternation of both elements [37]. Moreover, the detected upper limit of about 12 doped silicon atoms could correspond to their arrangement as pairs on the opposite corners of the square faces. On the other hand, their distribution over the 12 cycles of the fullerene network is unlikely to be due to the experimental and theoretical results on, for instance, $C_{2n-2}Si_2^+$ clusters. In order to check this hypothesis, some experiments are planned for getting rid of mass coincidences, a problem that conceals most of the information in mass spectra.

References

1. H.W. Kroto *et al.*: Nature **318**, 162 (1985)
2. W. Krätshmer *et al.*: Nature **347**, 354 (1990)
3. J.R. Heath *et al.*: J. Am. Chem. Soc. **107**, 7779 (1985)
4. Y. Chai *et al.*: J. Chem. Phys. **95**, 7564 (1991)
5. L.M. Roth *et al.*: J. Am. Chem. Soc. **113**, 6298 (1991)
6. Y. Huang, B.S. Freiser: J. Am. Chem. Soc. **113**, 9418 (1991)
7. D.E. Clemmer *et al.*: Nature **372**, 248 (1994)
8. W. Branz *et al.*: J. Chem. Phys. **109**, 3425 (1998)
9. U. Zimmermann *et al.*: Phys. Rev. Lett. **72**, 3542 (1994)
10. T. Guo, C. Jin, R.E. Smalley: J. Chem. Phys. **95**, 4948 (1991)
11. H.-J. Muhr, R. Nesper, B. Schnyder, R. Kötz: Chem. Phys. Lett. **249**, 399 (1996)
12. T. Pradeep, V. Vijayakrishnan, A.K. Santra, C.N.R. Rao: J. Phys. Chem. **95**, 10 564 (1991)
13. J.F. Christian, Z. Wan, S. Anderson: J. Phys. Chem. **96**, 10 597 (1992)
14. R. Yu *et al.*: J. Phys. Chem. **99**, 1818 (1995)
15. J.C. Hummelen *et al.*: Science **269**, 1554 (1995)
16. F. Chen, D. Singh, S.A. Jansen: J. Phys. Chem. **97**, 10 958 (1993)
17. N. Kurita, K. Kobayashi, H. Kumahora, K. Tago: Phys. Rev. B **48**, 4850 (1993)
18. K. Esfarjani, K. Ohno, Y. Kawazoe: Phys. Rev. B **50**, 17 830 (1994)
19. S.-H. Wang *et al.*: J. Phys. Chem. **99**, 6801 (1995)
20. W. Andreoni *et al.*: J. Am. Chem. Soc. **118**, 11 335 (1996)
21. T. Pichler *et al.*: Phys. Rev. Lett. **78**, 4249 (1996)
22. S. Haffner *et al.*: Eur. Phys.J. B **1**, 11 (1998)
23. N. Kurita *et al.*: Chem. Phys. Lett. **198**, 95 (1992)
24. W. Andreoni, F. Gygi, M. Parinello: Chem. Phys. Lett. **190**, 159 (1992)
25. T. Kimura, T. Sugai, H. Shinohara: Chem. Phys. Lett. **256**, 269 (1996)
26. J.L. Fye, M.F. Jarrold: J. Phys. Chem. **101**, 1836 (1997)
27. M. Pellarin *et al.*: Chem. Phys. Lett. 277, 96 (1197)
28. C. Ray *et al.*: Phys .Rev. Lett. **80**, 5365 (1998)
29. J.L. Vialle *et al.*: Rev. Sci. Instrum. **68**, 2312 (1997)
30. E.A. Rohlfing, D.M. Cox, A. Kaldor: J. Chem. Phys. **81**, 3322 (1984)
31. F. Tast *et al.*: Phys. Rev. Lett. **77**, 3529 (1996)
32. P.P. Radi *et al.*: J. Chem. Phys. **88**, 2809 (1987)
33. S.C. O'Brien *et al.*: J. Chem. Phys. **88**, 220 (1988)
34. P. Sheier *et al.*: Phys. Rev. Lett. **77**, 2654 (1996)
35. P.W. Fowler, D.E. Manolopoulos: *An Atlas of Fullerenes* (Clarendon, Oxford 1995)
36. D. Babic, N. Trinajstic: Chem. Phys. Lett. **237**, 239 (1995)
37. G. Seifert *et al.*: Chem. Phys. Lett. **268**, 352 (1997)